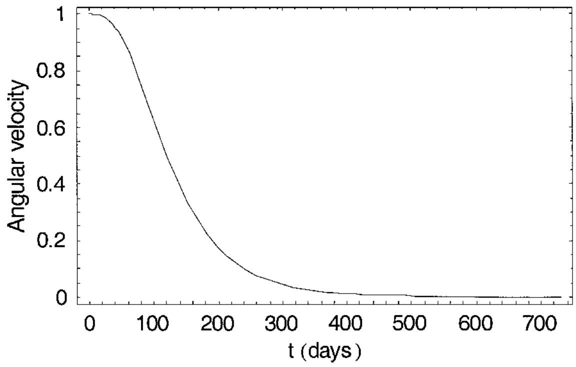

Fig. 4 Orbital angular velocity time history (normalized to initial orbital angular velocity).

V. Conclusions

A sail steering law has been derived in closed-form which transfers a solar sail with a lightness number $\beta = 1$ from a circular heliocentric orbit to a static equilibrium at the same heliocentric distance. The steering law is obtained as the solution to a first order ordinary differential equation, or is parameterized with respect to the solar sail polar angle. Independent of the starting orbit, it has been shown that the transfer angle for the maneuver is always $3\pi/4$.

Acknowledgment

This work was supported by the Leverhulme Trust.

Reference

[1]McInnes, C. R., *Solar Sailing: Technology, Dynamics and Mission Applications*, Springer-Verlag, London, 1999, pp. 118, 119.

Composite Estimate of Spacecraft Sensor Alignment Calibrations

Mark E. Pittelkau*
Johns Hopkins University, Applied Physics Laboratory, Laurel, Maryland 20723-6099

Introduction

Alignment Kalman filters (AKFs) for spacecraft sensor alignment calibration were developed in Refs. 1 and 2. There it was shown how to model attitude sensor misalignment and gyro calibration parameters and how to implement these models in a Kalman filter using the upper triangular diagonal (UD) factorization method of Bierman.[3] The efficacy of the calibration estimators in Refs. 1 and 2 was shown in simulation results using an attitude maneuver that makes all of the parameters observable.

Sensor alignment and calibration is of importance to the spacecraft community because the time and effort required for calibration is not trivial, calibration maneuvers could interfere with mission operation, and inadequate calibration can result in poor attitude knowledge and poor pointing performance. A problem in attitude sensor and gyro calibration is that a single attitude maneuver profile may not be sufficient to estimate all of the calibration parameters with small covariance because observability of the gyro parameters depends on the maneuver. Restrictions on such a maneuver may be due to physical, operational, or design constraints. The use of only one maneuver profile might also not be desirable because small thermal effects on alignment and gyro parameters could bias the calibration estimates. The constraints on the system considered in this Note are that no special calibration maneuvers be required and that calibration be performed using only normal Earth scanning maneuvers. Thermal distortion is the one of the drivers for the latter.

The objective of this Note is to introduce the technique of combining several estimated calibration parameter sets to obtain a composite least-squares estimate that has smaller covariance than all of the individual estimates. An algorithm is developed to compute the composite estimate from the estimated calibration parameter sets and the UD-factored covariances produced by the AKF. The algorithm utilizes the UD factors directly in a recursive, computationally efficient, and numerically reliable manner. It will be shown via simulation results that, with an appropriate set of attitude maneuvers, all parameters can be estimated with small covariance, even if some parameters (or linear combination of parameters) are of limited accuracy due to maneuver restrictions.

This idea of a composite estimator is not unlike the two-stage estimator in Ref. 4, where the final estimates from several executions of a first-stage estimator are used as measurements in a second-stage estimator.

A mathematical statement of the problem is given in the next section followed by the Kalman filter solution. Simulation results show the effectiveness of combining calibration parameter estimates that result from various maneuver scenarios. Results are shown for idealized maneuvers and for a set of realistic maneuvers for an Earth-imaging spacecraft.

Preliminaries

The AKFs reported in Refs. 1 and 2 produce a set of attitude, gyro bias, and calibration parameter estimates and the UD factors of the covariance matrix by processing attitude sensor data collected during a calibration maneuver. Let $\hat{\mathbf{x}}$ be the vector of estimated calibration parameters at the end of the calibration maneuver and let R be its covariance. The UD factors of R can be obtained directly from the UD factors of the covariance matrix $\boldsymbol{P}$ from the Kalman filter. There are $m = 6$ attitude perturbation and gyro bias states and n calibration parameters in the filter state vector. Partitioning $\boldsymbol{P}$ and its UD factors gives

$$
\begin{aligned}
\boldsymbol{P} &= \begin{array}{c} \overbrace{\phantom{P_{11}}}^{m}\ \overbrace{\phantom{P_{12}}}^{n} \\ \begin{bmatrix} \boldsymbol{P}_{11} & \boldsymbol{P}_{12} \\ \boldsymbol{P}_{21} & \boldsymbol{P}_{22} \end{bmatrix} \end{array} \begin{matrix} \}m \\ \}n \end{matrix} \\
&= \boldsymbol{UDU}^T \\
&= \begin{bmatrix} U_{11} & U_{12} \\ 0 & U_{22} \end{bmatrix} \begin{bmatrix} D_1 & 0 \\ 0 & D_2 \end{bmatrix} \begin{bmatrix} U_{11}^T & 0 \\ U_{12}^T & U_{22}^T \end{bmatrix} \\
&= \begin{bmatrix} U_{11}D_1U_{11}^T + U_{12}D_2U_{12}^T & U_{12}D_2U_{22}^T \\ U_{22}D_2U_{12}^T & U_{22}D_2U_{22}^T \end{bmatrix} \qquad (1)
\end{aligned}
$$

where $\boldsymbol{U}$ is unit upper triangular and $\boldsymbol{D}$ is diagonal. Thus $\boldsymbol{P}_{22} = U_{22}D_2U_{22}^T \triangleq R$, so that the UD factors of the parameter error covariance R are simply the partitions U_{22} and D_2 of the UD factorization of $\boldsymbol{P}$. If the UD factorization of $\boldsymbol{P}$ is stored in packed form, then the packed form of U_{22} and D_2 is extracted by skipping the first $m(m+1)/2 + mn$ elements of the packed UD factors of $\boldsymbol{P}$. To simplify notation in the developments that follow, let $U = U_{22}$ and $D = D_2$ so that $R = UDU^T$.

The AKF is run N times to process attitude and gyro data from each of N separate calibration maneuvers. Thus, we have N estimated calibration parameter vectors $\hat{\mathbf{x}}_1, \hat{\mathbf{x}}_2, \ldots, \hat{\mathbf{x}}_N$ and UD factors of the covariance matrices $R_1, R_2, \ldots, R_N$, each $\hat{\mathbf{x}}_k$ and R_k being the final value at the end of the AKF run. These estimates can be regarded as noisy observations $\boldsymbol{y}_1, \boldsymbol{y}_2, \ldots, \boldsymbol{y}_N$ of the true parameter

Received 4 December 2001; revision received 11 September 2002; accepted for publication 10 October 2002.

*Senior Professional Staff, Space Department; mittelkau@ieee.org. Senior Member AIAA.

vector $\boldsymbol{x}$, where the observation equation is given by

$$\boldsymbol{y}_k = \boldsymbol{x} + \boldsymbol{e}_k \tag{2}$$

where $\boldsymbol{e}_k$ is the estimation error. The measurement error covariance $\mathcal{E}\{\boldsymbol{e}_k\boldsymbol{e}_k^T\} = R_k$ is available in its UD-factored form as discussed earlier. ($\mathcal{E}\{\cdot\}$ is the expectation operator.) The composite estimator requires that $\mathcal{E}\{\boldsymbol{e}_k\boldsymbol{e}_\ell^T\} = \boldsymbol{0}$ for $k \neq \ell$, that is, that the $\boldsymbol{e}_k$ are independent. The error $\boldsymbol{e}_k$ is due to 1) the measurement noise during the AKF run, 2) the process noise during the AKF run, 3) the initial errors in the AKF states that are not included in the composite parameter vector (which is the initial attitude error), and 4) the initial calibration parameter estimate errors (including the initial gyro bias estimate errors). The following is a brief analysis of the independence of the $\boldsymbol{e}_k$.

The attitude measurement noise sequence $\{\boldsymbol{v}_i\}$ between and within each AKF run is independent. The process noise sequence $\{\boldsymbol{w}_i\}$ between and within each AKF run is also independent. It is also true that the $\boldsymbol{v}_i$ and $\boldsymbol{w}_j$ are independent for all i and j. Furthermore, the AKF runs are made with measurements from nonoverlapping intervals. The attitude estimate at the start of each AKF run is initialized with a measurement of attitude, so that the initial attitude estimate error is due only to the measurement noise, not the past process noise. This error is independent from one AKF run to another because the attitude measurement errors are independent. Therefore the components of $\boldsymbol{e}_k$ and $\boldsymbol{e}_\ell$ due to process noise are independent for $k \neq \ell$. Now we need to show that the error in the initial estimate of the calibration parameter vector at the start of the AKF run is independent of the initial estimate at the start of other runs. This true if the initial covariance is infinite, which says that the initial estimate contains no information and contributes nothing to the first and subsequent AKF updates, and in particular the final AKF estimate. Although an infinite initial parameter error covariance is not numerically achievable, it can be effectively achieved with a large initial covariance (at least three times the standard deviation of the precalibration parameters, which are considered to be random variables). When the initial parameter error covariance is large and the steady-state parameter error covariance is small (good observability), then the initial error does not weigh heavily in the final estimate error. Thus, the assumption that the initial estimate errors are uncorrelated is mild. In the case of poor observability, the covariance will remain large, and the estimate will contribute little to the composite estimate when other AKF runs have good observability. The effect of poor observability is discussed further at the end of the "Conclusions" section.

A model for the evolution of the constant parameter vector $\boldsymbol{x}$ is

$$\boldsymbol{x}_{k+1} = \boldsymbol{x}_k \tag{3}$$

The state transition matrix for this model is simply the identity matrix. Observe that there is no process noise in this model because $\boldsymbol{x}$ is constant. Our objective is to compute a minimum-variance composite estimate $\hat{\boldsymbol{x}}$ of $\boldsymbol{x}$ given the measurements and the UD factors of the error covariance matrices.

Kalman Filter Solution

A Kalman filter based on the measurement equation (2), and the state equation (3) can be used to obtain an estimate $\hat{\boldsymbol{x}}$ that is better than any of the measurements $\boldsymbol{y}_k$. The estimate error covariance will be updated by using the modified Agee–Turner algorithm for numerical stability and accuracy (see Ref. 3). This algorithm is based in part on the scalar measurement update method (this author's terminology). The technique comes from Ref. 5, where it is not given a name; also see the Appendix in Ref. 6. The scalar measurement update method requires that the measurement covariance matrix R_k be diagonal. Because R_k is not diagonal, a modification of the measurement equation (2) is made so that the resulting measurement error covariance is diagonal. From Eq. (2) and the UD factor U_k of $R_k = U_k D_k U_k^T$, we get

$$\begin{aligned}\bar{\boldsymbol{y}}_k &= U_k^{-1}\boldsymbol{y}_k \\ &= U_k^{-1}\boldsymbol{x} + U_k^{-1}\boldsymbol{e}_k \\ &= U_k^{-1}\boldsymbol{x} + \varepsilon_k \end{aligned} \tag{4}$$

with $\mathcal{E}\{\varepsilon_k\varepsilon_k^T\} = U_k^{-1}\mathcal{E}\{\boldsymbol{e}_k\boldsymbol{e}_k^T\}(U_k^{-1})^T = D_k$. Because D_k is diagonal, the elements of the error vector ε_k are mutually independent, and so the estimate $\hat{\boldsymbol{x}}_k$ and its covariance P_k can be iteratively updated with one element of $\bar{\boldsymbol{y}}$ at a time by using the scalar update method.

Note that because U_k is a square-root factor of R_k, it is far better conditioned numerically than R_k. A poorly conditioned U_k would be detected as a numerical problem during an AKF run and, therefore, would be eliminated from the composite estimate. Thus, we can assume that U_k is sufficiently well conditioned.

The observation matrix U_k^{-1} in Eq. (4) is easy to compute because U_k is unit upper triangular and can be computed in situ one row at a time. Each row of U_k^{-1} can be regarded as an observation matrix H_i for the scalar measurement $\bar{\boldsymbol{y}}_{k,i}$. The filter residual is given by $\bar{\boldsymbol{y}}_{k,i} - H_i\hat{\boldsymbol{x}}_{(i-)} = H_i(\boldsymbol{y}_k - \hat{\boldsymbol{x}}_{(i-)})$. The following C code fragment computes U_k^{-1}, the scalar measurement residual z_i, the updated estimate $\hat{\boldsymbol{x}}_{k_{(i)}}$, and the UD factors of the covariance $P_{k_{(i)}}$ of $\hat{\boldsymbol{x}}_{k_{(i)}}$:

```
for (i = 0; i < Ns; i++) {
  // VARIANCE OF OBSERVATION ERROR
  r = R[i][i] ;

  // OBSERVATION MATRIX inv(U)
  for (j = 0; j < i; j++) H[j] = 0.0 ;
  H[i] = 1.0 ;
  for (j = i+1; j < Ns; j++) {
     s = R[i][j] ;
     for (k = i+1; k < j; k++) s+= R[i][k]*R[k][j] ;
     R[i][j] = -s ;
     H[j] = R[i][j] ;
  }

 // RESIDUAL
 z = y[i] - x[i] ;
 for (j = i+1; j < Ns; j++) z += H[j]*(y[j] - x[j]) ;

 // STATE ESTIMATE AND COVARIANCE FACTOR UPDATE
 ageeturner(r, z, c, P, H, x, edit) ;
}
```

The `edit` variable indicates whether the measurement `z` has been edited according to the residual test threshold `c`. The array `R` contains the matrix U with D stored in its diagonal. `R` is overwritten with U_k^{-1} in situ by row. Each row of U_k^{-1} is also copied to `H` as it is computed. The array `P` contains the UD factors of the covariance matrix $P_{k_{(i)}}$. The code can be modified to avoid overwriting `R` with U_k^{-1} or to eliminate the storage for `H`. It might be important to overwrite `R` and `H` only for very large matrices.

The initial estimate $\hat{\boldsymbol{x}}_1$ is set equal to the first calibration estimate $\boldsymbol{y}_1$, and the UD factors of the initial covariance P_1 are set equal to the UD factors of R_1. The first update then proceeds with $\boldsymbol{y}_2$ and R_2. The modified Agee–Turner algorithm in the function `ageeturner` updates $\hat{\boldsymbol{x}}_{k_{(i)}}$ and the UD factors of $P_{k_{(i)}}$ with the measurement $\boldsymbol{y}_{k,i}$. This algorithm is too long to be given here, but its derivation and a FORTRAN implementation are given in Ref. 3. An algorithm for computing only the diagonal of the covariance matrix P_k from the UD factors is given in Ref. 6.

Generally it is said that a least-squares solution is less sensitive to unusually large measurement errors (outliers) than a Kalman filter estimate. This is an incorrect statement because the least-squares solution and the Kalman filter solution are identical once all of the measurements are processed. What the statement means to say is that outliers are easier to find in the least-squares residual than in the filter residuals when the filter has processed few of the measurements and has not converged. For this reason the `a posteriori` measurement residuals are computed in the algorithm above after the Kalman filter has processed all of the measurements. Outliers can then be identified, measurements edited, and the remaining measurements reprocessed.

Alternative Solution

One alternative to the approach presented is use the estimated parameters and their covariance from one maneuver to initialize the AKF for processing data from the next maneuver. This chained AKF method has the advantages 1) that the requirement for independence of the a priori estimates no longer applies, 2) that process noise on the parameters can be used to track variations in the parameters, and 3) that a separate program is not needed to produce the composite estimate.

At the start of each AKF run, the attitude estimate is initialized to the first attitude measurement and the remainder of the parameters are initialized to the estimate from the previous AKF run. The covariance is initialized with the covariance from the previous AKF run but with a reinitialization of the attitude error covariance and of the cross-covariance between attitude and the misalignment for the sensor used to initialize the AKF. The initial attitude covariance is the measurement error covariance plus the misalignment covariance of the attitude sensor that provided the attitude measurement. It is imperative to initialize correctly the cross covariance between the attitude error and the attitude sensor misalignment, otherwise the AKF will converge to the wrong estimate. The initialization of the covariance should be carried out directly on the UD factors of the covariance from the previous AKF run rather than the more obvious, expedient, and less accurate method of forming the covariance matrix from the UD factors, applying the modifications just described for initialization, and factoring the modified covariance. This initialization procedure is similar to the initialization of the first AKF run, which is described in Ref. 1.

Note that the order in which the data segments are processed is not important. A slight disadvantage of the chained AKF method is that part of the processing sequence needs to be repeated if subsequent analysis shows a problem with one of the links in the chain. The algorithm given in the preceding section is far more efficient in this regard. The chained AKF method has not yet been tested. Another alternative solution method is batch least-squares, but this offers no computational advantage.

Results

An AKF for estimating attitude, gyro bias, and various calibration parameters was derived in Ref. 1. The calibration parameter vectors are the nonorthogonal gyro axis misalignment $\boldsymbol{\xi}$, symmetric scale factors of the gyro $\boldsymbol{\lambda}$, asymmetric scale factors of the gyro $\boldsymbol{\mu}$, and misalignment of two star trackers $\boldsymbol{\delta}_{s1}$ and $\boldsymbol{\delta}_{s2}$. The payload alignment vector $\boldsymbol{\delta}_c$ is also modeled, but no payload measurements were processed for the results of this Note. The state vector and measurements vectors are $\boldsymbol{x} = \boldsymbol{y} = [\boldsymbol{\xi}^T, \boldsymbol{\lambda}^T, \boldsymbol{\mu}^T, \boldsymbol{\delta}_{s1}^T, \boldsymbol{\delta}_{s2}^T, \boldsymbol{\delta}_c^T]^T$. The fixed portion of the gyro bias could also be included in this parameter set. If the time between measurements $\boldsymbol{y}_i$ and $\boldsymbol{y}_{i+1}$ is sufficiently long such that the gyro bias due to angular random walk and rate random walk is uncorrelated, then the fixed bias of the gyro can also be estimated. An independent sequence of star tracker noise and gyro noise was generated for each of the calibration maneuvers defined subsequently so that the errors $\boldsymbol{e}_k$ are independent, with the exception of influence of the initial parameter estimate error and covariance; this will be remarked on further in the Conclusions section.

A sequence of three 1128-s planar calibration maneuvers are sinusoidal at an angular rate of 0.5 deg/s varying at 0.01 Hz in the x axis for the first maneuver, in the y axis for the second maneuver, and in the z axis for the third maneuver. These maneuvers are thus defined by the angular rate vectors,

$$\boldsymbol{\omega}_1 = (0.5\sin[2\pi(0.01)t], 0, 0)^T \tag{5a}$$

$$\boldsymbol{\omega}_2 = (0, 0.5\sin[2\pi(0.01)t], 0)^T \tag{5b}$$

$$\boldsymbol{\omega}_3 = (0, 0, 0.5\sin[2\pi(0.01)t])^T \tag{5c}$$

Another calibration maneuver consists of simultaneous nonharmonic sinusoidal angular rates in each body axis with peak amplitude of 1 deg/s and frequency of variation of 0.01, 0.009, and 0.008 Hz in the x, y, and z axes, respectively, that is, the angular rate vector is

$$\boldsymbol{\omega} = \begin{pmatrix} \sin[2\pi(0.010)t] \\ \sin[2\pi(0.009)t] \\ \sin[2\pi(0.008)t] \end{pmatrix} \tag{6}$$

This maneuver may be considered ideal in the sense that it is easy to generate and causes all of the parameters to converge in a reasonable amount of time and within the maneuver capability of the spacecraft. The time history of convergence of the calibration parameters for this maneuver was shown in Ref. 1.

The 1σ star tracker accuracy is 6 arc-s in the cross boresight axes and 37 arc-s in the boresight axis. The standard deviation of the rate white noise of the gyros is 0.005 deg/$\sqrt{}$h, and their 1σ drift stability is 0.05 deg/h over 1000 s. The star tracker data rate is 5 Hz, and the gyro data rate is 400 Hz. The filter update rate is 5 Hz. An independent noise sequence is generated for each maneuver and, of course, for each sensor. The gyro error model is described in Ref. 1. The star tracker error is simply a rotation error in the tracker frame, this error being independent white Gaussian noise in each axis. The gyro and star tracker measurements are passed through the AKF to produce an estimated calibration parameter vector for each maneuver.

The calibration results for these maneuvers are summarized in Table 1. The true values of the calibration parameters and their a priori standard deviation of error are shown in Table 2. As can be

Table 1 Individual and composite calibration estimates for sinusoidal maneuvers

		x-axis motion		y-axis motion		z-axis motion		Composite		Nonharmonic	
Parameter	Axis	Estimate	σ	Estimate	σ	Estimate	σ	Estimate	σ	Estimate	σ
	x	507.9	4.4	−123.3	1499.6	−95.4	1499.6	507.9	4.4	505.2	4.4
$\boldsymbol{\lambda}$, ppm	y	−194.2	1499.7	524.9	4.2	−212.4	1499.7	524.9	4.2	521.6	4.2
	z	−149.5	1499.7	−184.3	1499.8	527.8	4.3	527.8	4.3	531.3	4.2
	x	203.0	12.7	24.4	1499.9	14.3	1499.8	203.0	12.7	182.2	12.7
$\boldsymbol{\mu}$, ppm	y	4.4	1499.9	191.6	11.5	15.2	1499.9	191.6	11.5	184.5	11.0
	z	−22.0	1499.9	6.8	1499.9	226.5	12.0	226.4	12.0	195.0	11.0
	x	60.3	1492.2	−242.1	1494.9	−394.1	35.5	−398.9	1.2	−396.0	1.2
$\boldsymbol{\xi}$, arc-s	y	−30.3	1493.8	13.2	1495.5	−323.2	35.0	−300.6	1.2	−300.6	1.2
	z	−142.8	1494.4	−211.5	35.2	124.7	1494.7	−200.5	1.2	−200.1	1.2
	x	−14.2	17.6	−19.5	30.4	−12.4	34.7	−19.1	0.8	−19.9	0.9
$\boldsymbol{\delta}_{s1}$, arc-s	y	−25.0	17.9	5.8	30.2	−2.9	34.7	−20.1	0.8	−21.4	0.8
	z	12.8	25.1	1.2	25.1	5.3	36.3	19.6	0.9	17.9	1.0
	x	15.4	17.6	19.9	30.4	22.7	35.5	20.2	0.8	18.1	0.9
$\boldsymbol{\delta}_{s2}$, arc-s	y	14.3	17.9	−6.7	30.2	−2.7	35.5	19.3	0.8	19.3	0.9
	z	27.6	25.1	1.7	25.1	13.1	34.7	20.5	0.9	20.5	1.0

Table 2 Individual and composite calibration estimates for realistic maneuvers

		$N=1$		$N=3$		$N=5$			
Parameter	Axis	Estimate	σ	Estimate	σ	Estimate	σ	True value	Initial σ
	x	499.9	19.8	502.3	8.8	506.7	6.2	510	1500
$\boldsymbol{\lambda}$, ppm	y	511.5	12.4	525.0	5.3	523.9	4.0	520	1500
	z	495.3	43.3	526.8	8.3	524.8	6.0	530	1500
	x	197.0	28.7	191.3	11.3	198.2	8.4	200	1500
$\boldsymbol{\mu}$, ppm	y	195.3	14.1	197.0	9.1	195.9	7.1	200	1500
	z	191.9	35.9	214.2	10.6	208.1	7.6	200	1500
	x	−410.7	8.5	−399.5	1.7	−400.2	1.2	−400	1500
$\boldsymbol{\xi}$, arc-s	y	−297.4	9.6	−298.1	2.0	−297.4	1.4	−300	1500
	z	−196.0	4.6	−199.4	1.8	−198.4	1.3	−200	1500
	x	−18.1	3.3	−20.6	1.5	−20.3	1.0	−20	60
$\boldsymbol{\delta}_{s1}$, arc-s	y	−22.9	3.3	−22.2	1.4	−22.3	1.1	−20	60
	z	22.6	3.0	20.0	1.4	21.0	1.0	20	60
	x	22.4	3.5	19.3	1.4	19.8	1.1	20	60
$\boldsymbol{\delta}_{s2}$, arc-s	y	23.4	2.9	22.1	1.4	22.3	1.0	20	60
	z	23.6	3.2	20.7	1.4	21.0	1.1	20	60

seen in Table 1, only some of the parameters are identifiable in each of the three planar maneuvers. The standard deviation of error of the unidentifiable parameters remain close to their a priori value. As shown in Table 1, the composite estimate computed from the three calibrations using the individual planar maneuvers results in estimates that are close to the true values and that have small standard deviations of error. Similar results are also shown for the more nearly ideal nonharmonic sinusoidal maneuver. This suggests that certain permissible nonideal maneuvers may be substituted for an optimal calibration maneuver that might not be permissible or desirable.

A sequence of five realistic (but simulated) maneuvers for an agile Earth-imaging spacecraft were used to produce the results that are summarized in Table 2. These maneuvers range from 200 to 600 s in length and were generated by scanning various swaths of the Earth during separate imaging events. A set of star tracker and gyro measurements is generated by a spacecraft simulator for each maneuver. These measurements are passed through the AKF to produce five estimated calibration parameter vectors, which are numbered 1–5. The results shown in Table 2 are the calibration parameter vector 1 ($N=1$) and the composite estimate of calibration parameter vectors 1–3 ($N=3$) and of calibration vectors 1–5 ($N=5$). The corresponding standard deviation of error is also shown in Table 2. For $N=1$, the standard deviation is computed from the UD factors of the AKF covariance; for $N>1$, it is computed from the UD factors of the composite estimate covariance. As can be seen for the solitary maneuver ($N=1$), the parameters are only partially identifiable, that is, their standard deviation of error decreased but not nearly to the values achieved with the "ideal" nonharmonic maneuver Eq. (6), and the parameter estimates did not converge close enough to the true parameters. This is due to the lack of sufficient maneuvering in all axes and is typical of all realistic spacecraft maneuvers during normal uninterrupted operation. As can be seen, the composite estimate improves as the number of calibration maneuvers increases. The composite estimate of parameter estimates from five calibration maneuvers ($N=5$) is much improved over the estimate from the solitary maneuver ($N=1$). None of the individual maneuvers by itself was "rich" enough to identify all of the parameters with small standard deviation of error.

Conclusions

The problem of limited calibration performance due to calibration maneuver limitations was addressed. The technique introduced to solve this problem may also be used to make operational requirements less demanding with regard to the maneuvers required for spacecraft sensor alignment and calibration. The technique is to combine in a least-squares sense the calibration estimates from various calibration scenarios into a composite estimate, where each scenario may be insufficient to estimate all of the calibration parameters well. The Kalman filter algorithm developed to compute the composite estimate operates directly on the already-available UD factors of the measurement covariance matrix to maximize numerical stability and accuracy and to minimize computation and storage. The algorithm is general and can be applied to any calibration set and the UD factors of its covariance matrix.

A word of caution is needed in applying the algorithm in this Note. The maneuvers used to produce the individual estimates must be "different enough" so that all of the parameters of the composite estimate converge with small standard deviation of error. Repeating the same maneuver several times is not helpful unless that maneuver provides full observability of the parameters. One requirement on the calibration maneuver that has not been proven but is easily demonstrated via simulation is that the angular rates in each axis be nonharmonically related.

The reader should also be aware that parameters that are not identifiable from a given sequence of maneuvers but that have a *finite* initial covariance at the start of each AKF run will exhibit a smaller covariance in the composite estimate. An infinite a priori covariance of the initial parameter estimates would theoretically avoid this problem, but is not numerically possible except in the square root information filter formulation.[3] This problem is not severe because unobservability is usually obvious. This was demonstrated in the data reported in this Note.

Acknowledgment

The author thanks reviewer 4 for a very thorough review, including his own analysis of the algorithm developed in this Note.

Reference

[1]Pittelkau, M., "Everything Is Relative in Spacecraft System Alignment Calibration," *Journal of Spacecraft and Rockets*, Vol. 39, No. 3, 2002, pp. 460–466.

[2]Pittelkau, M., "Kalman Filtering for Spacecraft System Alignment Calibration," *Journal of Guidance, Control, and Dynamics*, Vol. 24, No. 6, 2001, pp. 1187–1195.

[3]Bierman, G. J., *Factorization Methods for Discrete Sequential Estimation*, Academic Press, New York, 1981, pp. 76–81, 100, 101.

[4]Pittelkau, M. E., and Price, E. L., "Parameter Adaptive Gun Fire Control," Ninth Meeting of the Coordinating Group on Modern Control Theory, ARDEC, Picatinny Arsenal, NJ, Oct. 1989.

[5]Jazwinski, A. H., *Stochastic Processes and Filtering Theory*, Academic Press, 1970, New York, pp. 271, 272.

[6]Pittelkau, M., "A Factorization and Least-Squares Method for Multi-Pass Sensor Alignment Calibration," *Advances in the Astronautical Sciences*, Vol. 108, Pt. 1, American Astronautical Society, Springfield, VA, 2001, pp. 693–700.